JOURNAL OF GUIDANCE, CONTROL, AND DYNAMICS
Vol. 19, No. 2, March–April 1996

Stability Augmentation Design of a Large Flexible Transport Using Nonlinear Parameter Optimization

Greta N. Ward*
The Boeing Company, Seattle, Washington 98124-2207
and
Uy-Loi Ly†
University of Washington, Seattle, Washington 98195-2400

Flight control laws for commercial aircraft have traditionally been designed using classical methods. This is adequate for rigid statically stable airplanes controlled by mechanical and hydraulic means. The challenge increases as pitch stability is reduced and structural flexibility is increased. The practical application of modern linear quadratic methods to stability augmentation system synthesis for a large subsonic transport is demonstrated. Stability, robustness, handling qualities, and dynamic load requirements under discrete and random gusts are addressed. The approach evolves from the traditional linear quadratic regulator methods to the synthesis of robust low-order controllers of a given structure with parameter optimization. The design is accomplished with aeroelastic models at flight conditions ranging from a low-speed takeoff to a high-speed cruise with forward and aft center-of-gravity configurations.

Nomenclature

CAP = control anticipation parameter
C_{M_u} = pitch moment coefficient with respect to speed
C_{M_α} = pitch moment coefficient with respect to α equal to $\omega_{\text{nsp}}^2/n_{z\alpha}$
C^* = $q + kn_z$, where k is airplane dependent
c = aerodynamic chord
$E[\,]$ = expected value
L_t = turbulence scale length
$\mathcal{M}_{\text{sr}}$ = stabilizer root bending moment
$\mathcal{M}_{\text{wr}}$ = wing root bending moment
$n_{z\alpha}$ = normal acceleration per α
Q/Q_{ss} = normalized pitch rate
Q_{ss} = steady-state pitch rate to a step δ_e
q_{dyn} = dynamic pressure
T_d = $25c/V_{\text{TAS}}$
T_1 = phugoid period of Q/Q_{ss} ideal model
T_2 = pitch zero of Q/Q_{ss} ideal model
t_f = terminal time
$\bar{u}$ = phugoid target mode
V_{TAS} = true airspeed
W_p^i = scalar weight per cost function i
w_g = vertical gust
w_i = disturbance input to the ith synthesis model
$\dot{w}_g$ = vertical gust rate
α = angle of attack
δ_{col} = column deflection
δ_e = elevator deflection
$\dot{\delta}_e$ = elevator rate
ζ_{sp} = short-period damping ratio
ζ_t = damping ratio of short-period target zeros
η_g = white noise input of unit power spectral density
θ_c = impulse pitch command
θ_m = pitch response of Q/Q_{ss} ideal model
$\bar{\theta}$ = short-period target mode
$\sigma^2_{c_{1,2,3,4}}$ = bounds on covariance responses to von Kármán turbulence
$\sigma^2_{d_{1,2}}$ = bounds on covariance responses to discrete gust
σ_g = von Kármán turbulence rms intensity
τ = von Kármán turbulence model time constant, L_t/V_{TAS}
ω_d = discrete gust frequency, $2\pi/T_d$
ω_{nsp} = short-period natural frequency
ω_{ph} = phugoid target zero
ω_{sp} = short-period frequency of Q/Q_{ss} ideal model
ω_t = frequency of short-period target zeros

I. Introduction

THE design of robust control laws for a large, flexible, subsonic airplane with reduced static stability (RSS) is challenging in that there is a technological upper limit to the available control power. Given that the inertia I_{yy} of an airplane is proportional to the fifth power of its length (L^5) and the control power is only proportional to L^3, the control power to inertia ratio decreases with $1/L^2$. A length-constrained airplane with RSS will show a similar nonlinear decrease. The plane in this study indicated a $1/L^{1.5}$ relationship. RSS increases the demand on the actuation system, requiring a pitch stability augmentation system (PSAS). This PSAS is vital and must provide adequate stability, handling qualities, and robustness to variation in flight conditions and yet not unduly affect the structural dynamic loads (e.g., increase in wing root bending moment). This study addresses PSAS design for this type of subsonic airplane. Properly reduced aeroelastic models of the airplane have been developed for control synthesis. The complete PSAS design approach is based on optimal control.[1,2] This approach begins with the synthesis of linear quadratic regulator (LQR) designs satisfying all of the specified requirements without excessive control effort. These full-state solutions provide meaningful insight into achievable design characteristics and a direct way to evaluate the potential benefits of multivariable control. Yet LQR design is not practical since it requires all of the system states to be fed back. Consequently, low-order controllers based on specified output feedback structure are obtained with parameter optimization,[2] adopting the results from the LQR synthesis as guidelines. Detailed formulation of the design problem for parameter optimization is given in Sec. IV.

Received Nov. 28, 1994; presented as Paper 94-3590 at the AIAA Guidance, Navigation, and Control Conference, Scottsdale, AZ, Aug. 1–3, 1995; revision received Sept. 29, 1995; accepted for publication Oct. 30, 1995.

*Control Systems Engineer, Boeing Commercial Airplane Group, P.O. Box 3707; currently at Anderson Electric Controls, Inc., 8639 S. 212th Street, Kent, WA 98031. Member AIAA.
†Associate Professor, Department of Aeronautics and Astronautics, P.O. Box 352400. Member AIAA.

II. Problem Statement

A. Problem Description

The objective of this study is to develop a unified procedure for designing a PSAS for a large subsonic transport. The PSAS controller structure is based on feeding back C^*(Ref. 3). The design is accomplished with linear aeroelastic models that include the effect of unsteady aerodynamics.[4] The airplane also exhibits RSS behavior. Hence, a PSAS is required for acceptable handling qualities while keeping the structural dynamic loads of the aircraft within reasonable limits.

B. Background

Early work on active control of a transport airplane[5] demonstrated the potential benefits of multivariable control based on a linear quadratic Gaussian (LQG) method. Nevertheless, implementation of LQG control laws still poses a major challenge in terms of its dimensionality and the difficulty in addressing many design conditions through gain scheduling. In this study, practical PSAS design is addressed through a combination of LQR synthesis[1] and direct parameter optimization.[2] The LQR full-state feedback design is optimum with respect to a weighted sum of mean square responses to either random initial conditions or random white noise disturbances. In addition, the design has a guaranteed robustness of at least -6 dB–∞ in gain margin and ± 60 deg in phase margin. Although full-state feedback cannot be implemented in practice, the achieved performance and robustness can be used as a point of reference to identify the maximum level of improvement that can be obtained with an output-feedback control law of a particular structure. The LQR method also provides a timely assessment on preliminary design issues such as the required control activity and bandwidth to meet stability and performance objectives.[5]

Once optimal LQR PSAS designs are obtained, low-order controllers are synthesized via direct optimization[2,6] in an attempt to recover the same performance and robustness. The control-law structure can be arbitrary; however, this study adopted the C^* control concept.

C. Design Requirements

The PSAS must meet the following stability and handling qualities requirements. 1) The normalized pitch rate response Q/Q_{ss} to a step elevator input shall be between the appropriate lower and upper limits. 2) The short-period damping ratio ζ_{sp} shall be between 0.4 and 0.8. 3) The control anticipation parameter CAP must be within limits (i.e., $0.16 < CAP < 3.6$ for takeoff, approach, and landing, and $0.085 < CAP < 3.6$ for climb, cruise, and descent). This requirement translates into limits on the minimum and maximum acceptable ω_{sp}.

In addition, the design must possess robustness of at least 6 dB in gain margin and 45 deg in phase margin. While improving the pitch stability, the design must not degrade the basic aeroelastic stability nor increase the total gust loads. The requirements for these dynamic loads are based on not-to-exceed values obtained with preliminary structural analysis.

D. Design Models

For control-law synthesis, design models must include the effects of RSS as well as aeroelasticity. Structural models that include the effects of unsteady aerodynamics[4] had been developed for this purpose. These high-order models of approximately 240 states must be reduced for control system design. This reduction is accomplished via the LK reduction method,[7] which preserves the dominant modal characteristics over a wide range of frequencies as well as the steady-state behavior. As a result, models of approximately 40 states are obtained for the flight conditions listed in Table 1.

Open-loop analysis indicates a degenerate short-period mode. This occurs when the static margin (defined by C_{M_α}) is reduced. The exact effect on the resulting short-period and the phugoid modes is determined by the speed-stability term C_{M_u}.[8–10] In general, the short-period mode coalesces with the phugoid mode to form a pair of real roots (a degenerate short-period mode) and a highly damped oscillatory third mode. This behavior is shown in Fig. 1 corresponding to flight conditions 1 and 2 (Table 1). Note that the forward c.g. condition indicates an oscillatory short period within the required

Table 1 Design flight conditions

Flight condition	Description	q_{dyn}, psf	c.g., % mac
1	Takeoff	97.4	13.5
2	Takeoff	97.4	36.0
3	Cruise	269	13.5
4	Cruise	269	36.0

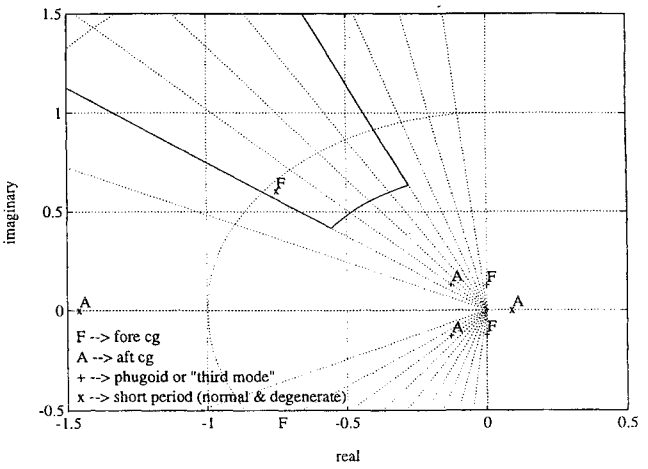

Fig. 1 Aft center-of-gravity effects on the short-period and phugoid modes, open loop configuration.

CAP and ζ_{sp} region, whereas the aft c.g. condition does not. Consequently the PSAS must move the short-period mode to this region to meet handling qualities requirements.

III. LQR Synthesis of PSAS

A. LQR Synthesis Model

For LQR design a model must be synthesized to encompass the requirements defined in Sec. II.C. First, the aeroelastic model must be rendered both minimal and balanced. The objective is to improve the numerical conditioning in terms of controllability and observability and also to remove all of the weakly controllable and weakly observable modes. Note that only a stable model can be balanced. The unstable or purely imaginary poles, if they exist, must first be isolated from the model to be balanced. This can be done by modal residualization.[5] A balanced realization can then be obtained for the stable part of the model. Nearly uncontrollable and unobservable modes are at the same time removed using the method of balanced truncation.[11] The unstable modes are subsequently appended back to produce the complete model for LQR synthesis. Integrators for the vertical, lateral, and longitudinal displacements (often present in structural models) are also removed as they do not contribute to the overall design problem and could pose numerical problems with the Riccati solution during LQR design. Moreover, these additional poles at the origin could lead to a system with degenerate roots at the origin, hindering the numerical diagonalization scheme in the design package SANDY.[6] This situation would occur when examining aircraft responses to a step input at the elevator column transducer or in the pitch command q_c.

Additional disturbance and ideal command models are also appended to the synthesis model. They are listed as follows.

1) A third-order filter for the transverse von Kármán turbulence model is given by

$$\frac{w_g(s)}{\eta_g(s)} = \frac{\sigma_g(1+2.618\tau s)(1+0.12981\tau s)}{(1+2.083\tau s)(1+0.832\tau s)(1+0.08977\tau s)} \tag{1}$$

where τ, σ_g, and the disturbance input η_g are as defined in the Nomenclature. Inclusion of this model ensures that the LQR design provides the desired disturbance attenuation to the von Kármán gust.

2) A second-order ideal model for Q/Q_{ss} is of the form

$$\frac{\theta_m(s)}{\theta_c(s)} = \frac{\omega_{sp}^2(1+T_2 s)}{\left(s^2+2\zeta_{sp}\omega_{sp}s+\omega_{sp}^2\right)(T_1 s+1)} \tag{2}$$

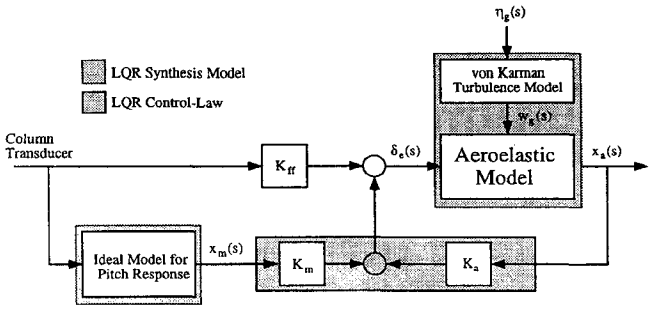

Fig. 2 Closed-loop system, LQR.

where ζ_{sp}, ω_{sp}, T_1, and T_2 are design parameters describing the desired pitch response to an impulse input $\theta_c(s)$. Note that T_1 was selected to be 100 s to reflect the slowly decaying pitch response in the speed-free model.

3) A first-order ideal model could also be set up for the speed variable u. Speed stability, however, was not a consideration for this study; hence, we assume $u_m(t) \equiv 0$.

Formulation of the synthesis model is done using state-space methods.[5] A diagram of this model is shown in Fig. 2.

B. LQR Synthesis

The LQR synthesis is based on the following cost function:

$$J_{LQ} = \int_0^\infty \left[y_c^T(t) Q y_c(t) + R\delta_e^2(t)\right] dt \tag{3}$$

which, according to Parseval's theorem, can be rewritten as

$$J_{LQ} = \frac{1}{2\pi}\int_0^\infty \left[y_c^*(j\omega) Q y_c(j\omega) + R\delta_e^*(j\omega)\delta_e(j\omega)\right] d\omega \tag{4}$$

The criterion variables are 1) $y_{c_1} = \bar{\theta} = (s^2 + 2\zeta_t\omega_t s + \omega_t^2)[\theta(s) - \theta_m(s)]$ = short-period target mode, 2) $y_{c_2} = \mathcal{M}_{sr}$ = stabilizer root bending moment, and 3) $y_{c_3} = \mathcal{M}_{wr}$ = wing root bending moment, and Q is a diagonal weighting matrix. The first criterion variable forms the appropriate target transmission zeros. The target zeros are totally defined by the parameters ω_t and ζ_t. Increasing the penalty weight on $\bar{\theta}$ moves the resultant closed-loop poles asymptotically toward these target zeros. Additional weights on y_{c_2} and y_{c_3} are carefully introduced to improve the loads, if necessary. Note that in this case there is only one control variable, the elevator $\delta_e(t)$.

The derived closed-loop system is shown in Fig. 2. The feedforward controller (gains K_{ff} and K_m) is in part accomplished by including the ideal model into the synthesis model. The resultant control law as indicated in Fig. 2 is

$$\delta_e(t) = K_a x_a(t) + K_m x_m(t) + K_{ff}\delta_{col}(t) \tag{5}$$

where $x_a(t)$ are the airplane and turbulence model states and $x_m(t)$ are the ideal model states. Note that K_{ff} is not directly obtained with LQR synthesis. Instead, K_{ff} is selected afterwards via direct simulation; its value is adjusted until the actual Q/Q_{ss} closely matches the desired response.

Design gains at each flight condition are obtained following an iterative procedure. First, penalty weights are chosen for the criterion y_{c_2} and control δ_e along with the parameters (ω_t, ζ_t) for the short-period target zeros. At some flight conditions, RSS makes it necessary to reduce ζ_t to a small value to attract the short-period mode away from the real axis, and thereby compensate for the increase in C_{M_α} (i.e., a loss in static margin).[9] In addition, since target zeros only attract the closed-loop poles in the asymptotic sense, it is sometimes necessary to increase the frequency ω_t beyond what would be the desirable CAP to obtain good handling qualities (short-period placement and Q/Q_{ss}).

In addition, some cases require penalty weights on y_{c_3} and y_{c_4} to improve the load reduction to random gust. Increasing the elevator control weight R also reduces M_{sr} and M_{wr}. The mean square responses of dynamic loads, elevator rates, and displacements to von Kármán turbulence are evaluated by calculating the covariance with the Lyapunov matrix equation.

Table 2 LQ design parameters

		Criterion weights[a]			Target zeros		
FC	R	$\bar{\theta}$	$\mathcal{M}_{sr}$	$\mathcal{M}_{wr}$	ω_t	ζ_t	K_{ff}
1	4	0.5	1	1.8	1.5	0.7	−0.005
2	5	1	0	1	2.5	0.2	−0.03
3	25	0.1	0	5	2.5	0.9	−0.0035
4	30	0.5	110	10	2.2	0.1	−0.012

[a] $\mathcal{M}_{sr}$ and $\mathcal{M}_{wr} \times 10^{-14}$.

Table 3 Gain and phase margins

	LQR		C^*_{opt}	
FC	GM, dB	PM, deg	GM, dB	PM, deg
1	−58.34	99.35	(−56.2, 16.8)	79.8
2	∞	68.45	14.9	69.5
3	∞	107.32	(−58.8, 12.8)	82.1
4	∞	82.32	11.0	51.1

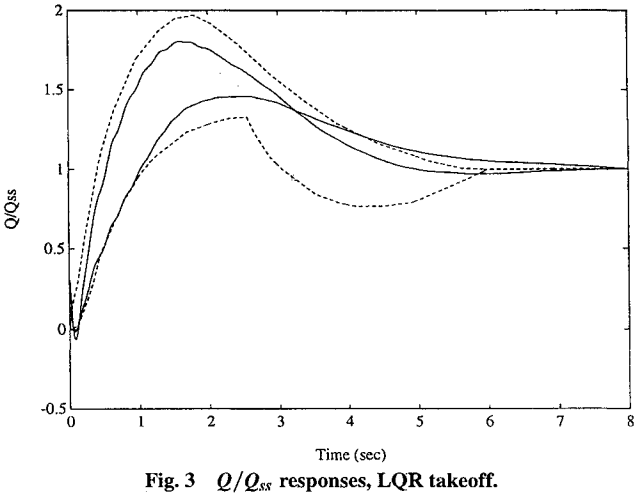

Fig. 3 Q/Q_{ss} responses, LQR takeoff.

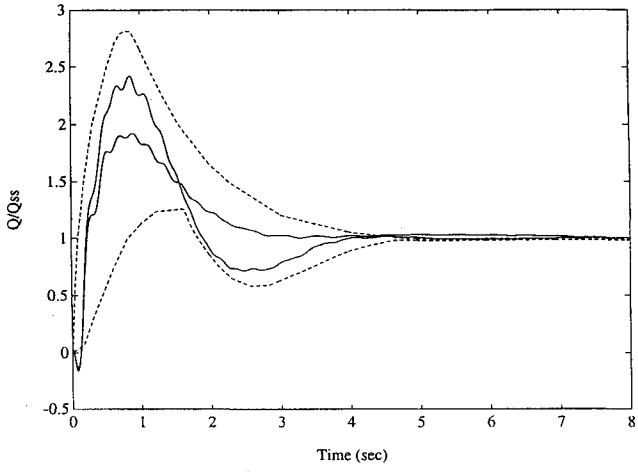

Fig. 4 Q/Q_{ss} responses, LQR cruise.

C. LQR Design Results

Design parameters in the LQR synthesis are summarized in Table 2. The achieved robustness in terms of gain and phase margins is shown in Table 3; clearly the results exceed the guaranteed robustness of (−6 dB, ∞) in gain margin and ±60 deg in phase margin. The Q/Q_{ss} compliance is shown in Figs. 3 and 4. The short-period damping and CAP compliance are shown in Figs. 5 and 6, respectively. Closed-loop dynamic loads, elevator rates and displacements are shown in Table 4 for random gusts and in Table 5 for discrete gusts.

IV. Control Synthesis Using Parameter Optimization

The LQR results indicate that a PSAS can achieve the desired stability, handling qualities and gust response. The next step is then

Table 4 $\mathcal{M}_{sr}$, $\mathcal{M}_{wr}$, δ_e, and $\dot{\delta}_e$ responses

	$\mathcal{M}_{sr}$, (10^6 in.-lb)		$\mathcal{M}_{wr}$, 10^6 in.-lb		δ_e, deg		$\dot{\delta}_e$, deg/s	
FC	LQR	C^*_{opt}	LQR	C^*_{opt}	LQR	C^*_{opt}	LQR	C^*_{opt}
1	2.76	2.71	5.97	7.49	1.11	1.88	3.56	4.10
2	5.30	5.49	8.81	9.03	1.60	1.96	7.17	5.94
3	12.4	12.4	20.0	20.2	1.98	3.11	9.10	12.2
4	14.5	14.6	21.0	20.1	2.18	2.22	15.5	16.0

Table 5 Peak $\mathcal{M}_{sr}$, $\mathcal{M}_{wr}$, δ_e, and $\dot{\delta}_e$, discrete gust

	% Reduction[a] $\mathcal{M}_{sr}$		% Reduction[a] $\mathcal{M}_{wr}$		δ_e, deg		$\dot{\delta}_e$, deg/s	
FC	LQR	C^*_{opt}	LQR	C^*_{opt}	LQR	C^*_{opt}	LQR	C^*_{opt}
1	−4.69	−2.67	1.34	−0.4	0.47	0.84	0.65	1.23
2	14.7	0	−2.18	0	1.12	1.56	1.17	2.56
3	21.2	4.90	−10.1	−11.0	3.25	4.28	10.4	18.1
4	4.48	21.1	−1.47	−4.33	1.36	3.26	6.27	15.3

[a]Compared to open-loop response.

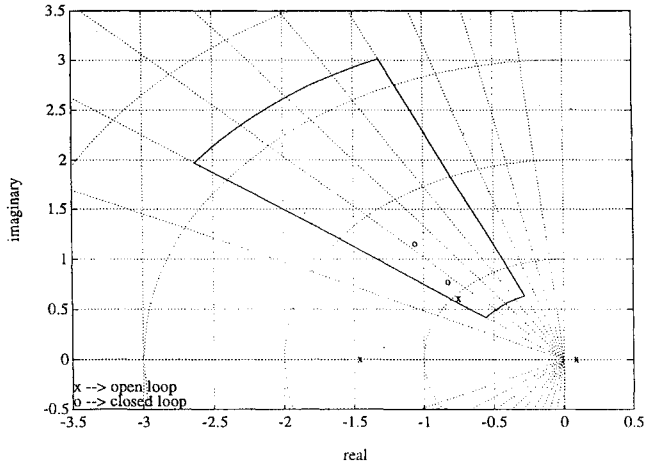

Fig. 5 Short-period damping and *CAP*, LQR takeoff.

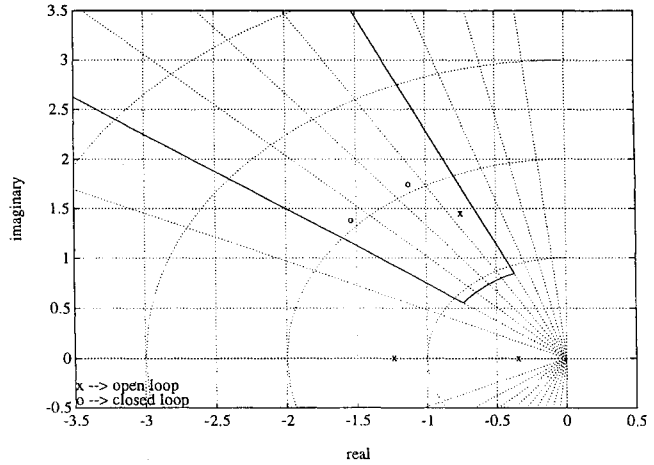

Fig. 6 Short-period damping and *CAP*, LQR cruise.

to realize such a control law in terms of an output-feedback design. One approach would be to synthesize a LQG control law[5] using the measurements of normal acceleration and pitch rate. The resulting controller, however, would be of high order (approximately 40th), and gain scheduling would be difficult. Hence, a simpler approach is attempted, which can only be done with direct parameter optimization.[6] Because of ongoing interest in the C^* criterion, a C^*-type controller was selected for the design optimization.

In this study, the design package SANDY[6] was used to solve for the optimum gains. The design algorithm behind SANDY is based on the optimization of a quadratic cost evaluated to a finite terminal time t_f. Given a linear time-invariant (LTI) system with impulse or white noise inputs, the objective is to find a LTI controller of a given structure and order such that the following performance index is minimized:

$$J = \sum_{i=1}^{N_p} W_p^i J^i\left(t_f^i\right) \tag{6}$$

where, for impulse inputs,

$$J^i\left(t_f^i\right) = \int_0^{t_f^i} \left[y_c^{iT}(t) Q^i y_c^i(t) + u^T(t) R^i u(t)\right] \mathrm{d}t \tag{7}$$

and for white noise inputs,

$$J^i\left(t_f^i\right) = E\left[y_c^{iT}\left(t_f^i\right) Q^i y_c^i\left(t_f^i\right) + u^T\left(t_f^i\right) R^i u\left(t_f^i\right)\right] \tag{8}$$

The design optimization may also include additional linear and nonlinear constraints: direct bounds on the design gains, eigenvalue constraints on the maximum real part and minimum damping, and covariance constraints on the control and criterion variables.

Note in Eq. (6) that J involves the sum of quadratic performance indices with the associated scalar weights $W_p^i(\geq 0)$. Individual performance index $J^i(t_f^i)$ is formulated to represent a particular design specification (Table 2). Thus, at each flight condition, we have $N_p = 3$ and the following objective function:

$$J = \sum_{i=1}^{3} J^i\left(t_f^i\right) \tag{9}$$

The design approach in SANDY provides the following advantages.

1) The initial guess for the controller need not be stable because the terminal time is finite. Closed-loop stability is guaranteed upon convergence using eigenvalue constraints.

2) Nonlinear and tracking requirements may be approximated using synthesis filters with a finite terminal time.

3) The computer program NPSOL is used to optimize the controller parameters for a minimum J.

4) Numerical optimization is efficient since gradients are evaluated analytically. The problem is, however, generally nonconvex, and the optimal design corresponds only to a local minimum.

A. Synthesis Models for Parameter Optimization

Given the three design criteria shown in Table 6, synthesis models are formulated as shown in Fig. 7. Note the differences from the LQR synthesis model (Fig. 2). This is a result of the different types of disturbance and command inputs used to evaluate the design specifications. Note that all of these models share the same control input and sensor outputs. These models and the associated design cost and constraint functions are as follows.

1. Synthesis Model 1 (Fig. 7)

To achieve handling qualities in the form of Q/Q_{ss}, an ideal model is formulated for the desired pitch rate response $q_m(t)$. The step input is modeled as the output of a first-order impulse filter with

Table 6 Formulation of synthesis models

Synthesis model	t_f, s	Disturbance, $w(t)$	Criterion, $y_c(t)$
1	10	$w_1(t)$ = impulse	$\Delta\dot{q}(t)$
Pitch command			$\Delta q(t)$
2	T_d	$w_2(t)$ = impulse	$M_{sr}(t)$
Discrete gust			$M_{wr}(t)$
			$\delta_e(t)$
			$\dot{\delta}_e(t)$
3	∞	$w_3(t)$ = white noise	$M_{sr}(t)$
von Kármán turbulence			$M_{wr}(t)$
			$\delta_e(t)$
			$\dot{\delta}_e(t)$
			$\dot{\theta}(t)$

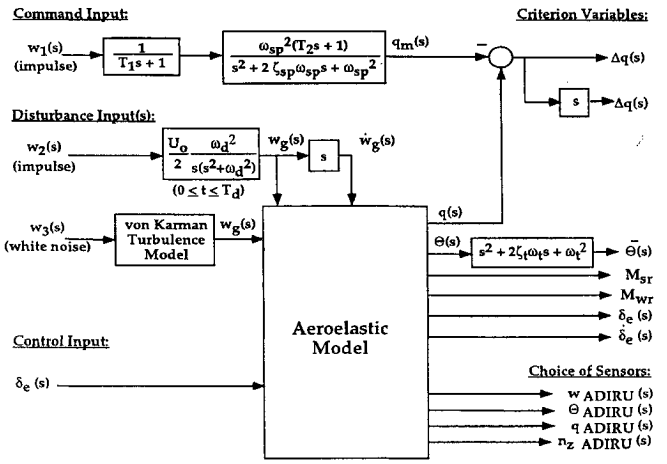

Fig. 7 Synthesis models 1, 2, and 3; direct optimization.

a slow time constant $T_1 = 100$ s. Note that the input to this filter corresponds to $w_1(s)$. Parameters T_2, ω_{sp}, and ζ_{sp} in the second-order filter are determined to produce a nominal response that lies between the required lower and upper boundaries of the Q/Q_{ss} envelope. Note that these parameters do vary with flight conditions. For the low-speed conditions: $T_2 = 2.0$ s, $\omega_{sp} = 1.0$ rad/s, and $\zeta_{sp} = 0.57$. For the high-speed conditions: $T_2 = 1.25$ s, $\omega_{sp} = 2.0$ rad/s and $\zeta_{sp} = 0.6$.

Alternately, a second-order approximation of the pitch response in the closed-loop LQR design may be used for this model. This is accomplished with SANDY using a model-matching technique. The ideal model then represents a solution that satisfies all requirements, regardless of the pitch zero and the degree of RSS. The design objective for synthesis model includes pitch rate and pitch acceleration tracking errors between the airplane and the ideal model. The resulting cost function is of the following form:

$$J^1(t_f^1) = \int_0^{t_f^1} \left\{ Q_1^1 \Delta q^2(t) + Q_2^1 \Delta \dot{q}^2(t) \right\} dt \tag{10}$$

2. Synthesis Model 2 (Fig. 7)

To address the airplane response to a discrete gust of the form

$$w_g(t) = \begin{cases} \frac{1}{2} U_o (1 - \cos \omega_d t) & t \le T_d \\ 0 & t > T_d \end{cases} \tag{11}$$

where $\omega_d = 2\pi / T_d$ and $T_d = 25c / V_{TAS}$, a synthesis model is formulated as shown in Fig. 3. Note that exciting the given third-order filter with an impulse input $w_2(s)$ will result in a sinusoidal output identical to the discrete gust for $0 \le t \le T_d$. The period T_d is adequate to capture the peak response to the discrete gust in Eq. (11), since the peak response is expected to occur between the time at maximum excitation ($t = T_d/2$) and where the gust excitation is removed ($t > T_d$). The output covariance response evaluated over the gust period T_d can be used to provide a rough measure to the maximum discrete gust loads. Given the low-frequency content of the gust excitation, if the output covariance is constrained to be small, then it is likely that the maximum discrete gust loads will also not be excessive. This synthesis model has the following cost function:

$$J^2(t_f^2) = \int_0^{t_f^2} \left\{ Q_1^2 M_{sr}^2(t) + Q_2^2 M_{wr}^2(t) \right\} dt \tag{12}$$

with additional direct constraints on the covariance responses

$$\int_0^{t_f^2} M_{sr}^2(t)\, dt \le \sigma_{d_1}^2$$
$$\int_0^{t_f^2} M_{wr}^2(t)\, dt \le \sigma_{d_2}^2 \tag{13}$$

and with terminal time $t_f^2 = T_d$. The criterion weights Q_1^2 and Q_2^2 and the upper bounds in the covariance constraints are selected iteratively until the resulting peak bending moment responses are below the allowable limits. Care must be taken in the selection of the upper bounds in Eq. (13) so as to not overly constrain the design problem where no feasible design solution exists.

3. Synthesis Model 3 (Fig. 7)

The dynamic loads and the elevator activity under a continuous von Kármán turbulence are accounted for in synthesis model 3 through the disturbance input $w_3(s)$. The short-period damping and CAP requirements are also included in the objective function using a short-period target mode with the desired damping ζ_t and frequency ω_t. Target zeros in a frequency-shaped cost function are only approached in the steady-state design, i.e., with the terminal time $t_f^3 \to \infty$. The design objective function is of the form

$$J^3(t_f^3) = Q_1^3 E\left[\bar{\theta}^2(t_f^3)\right] + Q_2^3 E\left[M_{sr}^2(t_f^3)\right] + Q_3^3 E\left[M_{wr}^2(t_f^3)\right] \tag{14}$$

with additional direct constraints on the covariance responses

$$E\left[M_{sr}^2(t_f^3)\right] \le \sigma_{c_1}^2, \qquad E\left[M_{wr}^2(t_f^3)\right] \le \sigma_{c_2}^2$$
$$E\left[\delta_e^2(t_f^3)\right] \le \sigma_{c_3}^2, \qquad E\left[\dot{\delta}_e^2(t_f^3)\right] \le \sigma_{c_4}^2 \tag{15}$$

The upper bounds are usually determined from either the open-loop responses or from the closed-loop responses of a baseline design. Starting with a reasonably small t_f^3, the terminal time t_f^3 is gradually increased until a steady-state solution is achieved[6] in the mean square response calculation.

V. C^* Control-Law Structure for Parameter Optimization

The C^* control-law structure for this study is shown in Fig. 8. Any feedback variables to be integrated are replaced by their integrated states to avoid uncontrollable poles at the origin in the feedback path. The feedforward and C^* augmentation gains are optimized simultaneously with respect to the overall performance index J given in Eq. (9) while subject to all of the nonlinear constraints defined in Eqs. (13) and (15). Table 7 shows the design parameters selected for the synthesis of the optimal C^* controller. The achieved robustness in terms of gain and phase margins is shown in Table 3 that surpasses the requirements of 6 dB in gain margin and 45 deg in phase margin. The Q/Q_{ss} compliance is shown in Figs. 9 and 10 for the takeoff and cruise conditions, respectively. Note that the pitch response is within the desired envelope. The CAP and short-period damping compliance are shown in Figs. 11 and 12. Closed-loop

Table 7 Design parameters in C^*_{opt} synthesis

FC	Synthesis model 1	Synthesis model 2	Synthesis model 3
1	$Q_1^1 = 100$	$Q_1^2 = 600$	$Q_1^3 = 10$
	$Q_2^1 = 10^4$	$\sigma_{d_1}^2 = 6.31 \times 10^{12}$	$\omega_t = 2.0$
	$\omega_{sp} = 1.0$		$\zeta_t = 0.7$
	$\zeta_{sp} = 0.57$		
	$T_2 = 2.0$		
2[a]	$Q_1^1 = 25$	$\sigma_{d_1}^2 = 18.982 \times 10^{12}$	$\omega_t = 2.0$
	$\omega_{sp} = 0.94$	$\sigma_{d_2}^2 = 2307.3 \times 10^{12}$	$\zeta_t = 0.7$
	$\zeta_{sp} = 0.62$		$\sigma_{c_1}^2 = 30.138 \times 10^{12}$
	$T_2 = 2.67$		$\sigma_{c_2}^2 = 8147.5 \times 10^{12}$
3	$Q_1^1 = 100$		$Q_1^3 = 10$
	$Q_2^1 = 10^4$		$\omega_t = 2.0$
	$\omega_{sp} = 2.0$		$\zeta_t = 0.9$
	$\zeta_{sp} = 0.6$		
	$T_2 = 1.25$		
4	$Q_1^1 = 1$		$Q_1^3 = 10$
	$Q_2^1 = 1$		$\omega_t = 2.0$
	$\omega_{sp} = 1.77$		$\zeta_t = 0.9$
	$\zeta_{sp} = 0.68$		$\sigma_{c_2}^2 = 48400 \times 10^{12}$
	$T_2 = 1.65$		

[a]Damping constraint of $\zeta_{sp} < 0.8$ was required to ensure a complex short-period mode.

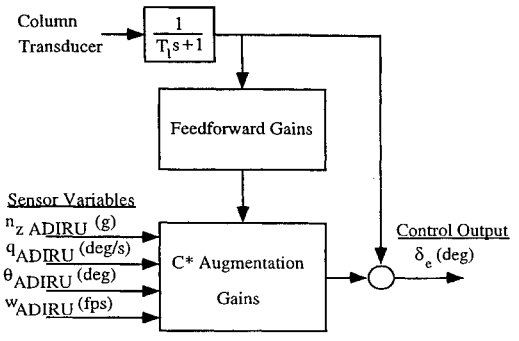

Fig. 8 C^* controller, direct optimization.

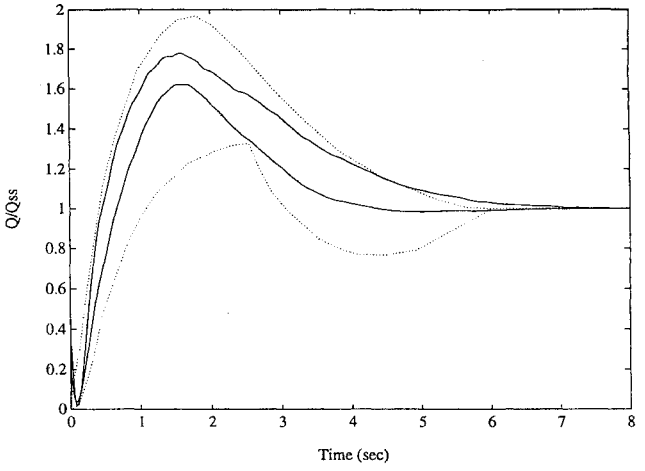

Fig. 9 Q/Q_{ss} responses, C^*_{opt} takeoff.

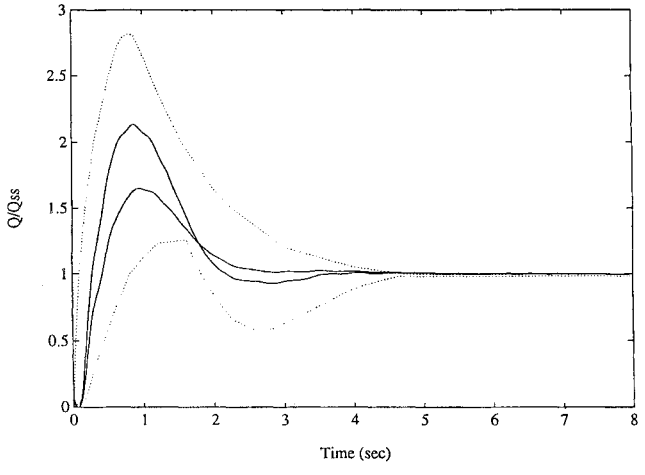

Fig. 10 Q/Q_{ss} responses, C^*_{opt} cruise.

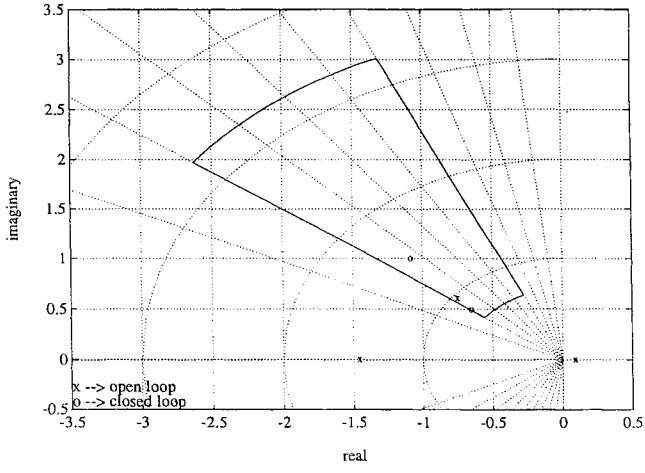

Fig. 11 Short-period damping and *CAP*, C^*_{opt} takeoff.

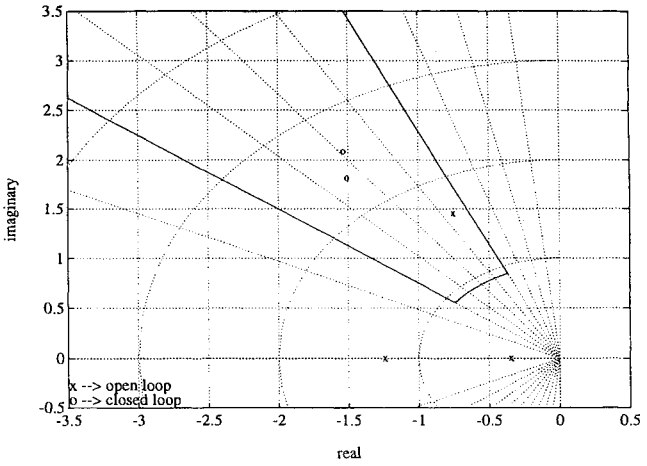

Fig. 12 Short-period damping and *CAP*, C^*_{opt} cruise.

dynamic loads as well as elevator rates and displacements are shown in Table 4 for random gusts, and in Table 5 for discrete gusts. Note that the design goals in terms of allowable loads and elevator activity are also met. The results obtained show the viability of parameter optimization for the design of a practical control law with a given structure. The potential of this approach is its ability to explore other types of stability augmentation systems for a large subsonic transport beyond the proposed C^* controller.

VI. Conclusions

Optimal control synthesis of a stability augmentation system for a large subsonic transport has been presented. A systematic design procedure has been developed that includes pertinent design requirements in the quadratic cost function with a frequency-shaped cost and a model-following method. Both feedback and feedforward design has been successfully obtained with the well-known LQR synthesis. The reduced-order implementation in the form of a C^* control law is designed with parameter optimization. The proposed numerical optimization-based method offers a convenient and powerful means of synthesizing practical control laws that approach the optimum performance and robustness of the LQR design using direct nonlinear constraints.

References

[1]Anderson, B. D. O., and Moore, J. B., *Optimal Control: Linear Quadratic Methods,* Prentice–Hall, Englewood Cliffs, NJ, 1990.

[2]Ly, U., Bryson, A. E., and Cannon, R. H., "Design of Low-Order Compensators Using Parameter Optimization," *Automatica*, Vol. 21, No. 3, 1985, pp. 315–318.

[3]Tobie, H. N., Elliott, E. M., and Malcom, L. G., "A New Longitudinal Handling Qualities Criterion," *Proceedings of National Aerospace Electronics Conference* (Dayton, OH), 1966.

[4]Roger, K. L., "Airplane Math Modeling Methods for Active Controls Design," AGARD-CP-228, Aug. 1977.

[5]Gangsaas, D., and Ly, U., "Application of a Modified Linear Quadratic Design to Active Control of a Transport Airplane," AIAA Paper 79-1746, Aug. 1979.

[6]Ly, U., "A Design Algorithm for Robust Low-Order Controllers," Dept. of Aeronautics and Astronautics, SUDAAR No. 536, Stanford Univ., Stanford, CA, Nov. 1982.

[7]Anderson, L. R., "Order Reduction of Aeroelastic Models Through LK Transformation and Riccati Iteration," AIAA Paper 93-3795, Aug. 1993.

[8]Etkin, B., *Dynamics of Flight-Stability and Control*, Wiley, New York, 1992, pp. 187, 188.

[9]McRuer, D., and Myers, T. T., "Flying Qualities of Relaxed Static Stability Aircraft, Volume II," TR-1178-1-I, Dept. of Transportation, Federal Aviation Administration Technical Center, Atlantic City Airport, NJ, Sept. 1982.

[10]Schuler, J. M., and Dahl, M. A., "Proposed Revisions to MIL-F-8785C Related to Flight Safety of Augmented Aircraft, Vol. II," Air Force Wright Aeronautical Labs., AFWAL-TR-82-3014, Wright–Patterson AFB, OH, April 1982, pp. 25–27.

[11]Pernebo, L., and Silverman, L. M., "Model Reduction via Balanced State Space Representations," *IEEE Transactions on Automatic Control*, Vol. AC-27, No. 2, 1982, pp. 382–387.